Few-cycle pulses from a graphene mode-locked all-fiber laser

D. G. Purdie,[1] D. Popa,[1,a)] V. J. Wittwer,[1] Z. Jiang,[1] G. Bonacchini,[1] F. Torrisi,[1] S. Milana,[1] E. Lidorikis,[2] and A. C. Ferrari[1]
[1]*Cambridge Graphene Centre, University of Cambridge, Cambridge CB3 0FA, United Kingdom*
[2]*Department of Materials Science and Engineering, University of Ioannina, Ioannina 45110, Greece*

(Received 7 April 2015; accepted 1 June 2015; published online 22 June 2015)

We combine a graphene mode-locked oscillator with an external compressor and achieve ~29 fs pulses with ~52 mW average power. This is a simple, low-cost, and robust setup, entirely fiber based, with no free-space optics, for applications requiring high temporal resolution. © *2015 AIP Publishing LLC*. [http://dx.doi.org/10.1063/1.4922397]

Ultrafast light pulses in the femtosecond range are needed for advanced photonics applications. E.g., in pump-probe spectroscopy, photophysical and photochemical relaxation processes are monitored by exciting a sample with an ultrashort light pulse. The maximum temporal resolution is determined by the duration, $\Delta\tau$, of the pulse. This is usually defined as the full width at half maximum (FWHM) of its intensity profile in the time domain, $I(t)$.[1] Alternatively, $\Delta\tau$ may be defined by the number of oscillation periods of the electric field carrier wave (optical cycles) within the pulse[2] $N = \frac{\Delta\tau}{T_0} = \nu_0\Delta\tau$, where T_0 is the optical cycle of frequency ν_0. The ultimate pulse duration is set by a single cycle of light, i.e., T_0, given by[2] $\frac{\lambda}{c}$, where λ is the wavelength and c is the speed of light. The uncertainty relation $\Delta\nu\Delta\tau \simeq \frac{1}{\pi}$ provides a measure of the minimum frequency bandwidth $\Delta\nu$ required to support an ultrashort pulse,[2] i.e., the broader the bandwidth, the shorter the supported pulse. In the visible and near infrared (NIR), T_0 lies, e.g., between 2 fs at $\lambda \sim 600$ nm and 5 fs at $\lambda \sim 1.5\,\mu$m, which set the ultimate speed limits for devices operating in this wavelength range. Achieving shorter pulses therefore requires moving to shorter wavelengths.

Pulses as short as 2-cycles can be generated directly from laser cavities using passive mode-locking.[1–3] Ti:Sapphire lasers are established tools for few-cycle pulse generation,[2] with the shortest pulses produced to date having $\Delta\tau \sim 5$ fs[4] at a centre wavelength, $\lambda_0 \sim 800$ nm, corresponding to less than 2-cycles, with spectral width $\Delta\lambda \sim 600$ nm.[4] Ti:Sapphire lasers able to generate few-cycle pulses are typically optimized to make use of the maximum $\Delta\lambda$ gain available.[2] Consequently, they have no wavelength tunability.[2] Tunable Ti:Sapphire lasers operate with longer pulse durations, e.g., $\Delta\tau \sim 150$ fs in a typical ~680–1080 nm commercially available spectral range.[5] Tunable few-cycle pulses can be achieved by exploiting nonlinear optical effects in optical parametric amplifiers (OPAs). These can be described by expressing the polarization (P) as a power series in the applied optical field (E):[6,7] $P = \epsilon_0[\chi^{(1)}E + \chi^{(2)}E^2 + \chi^{(3)}E^3 + ...]$, where ϵ_0 is the free space permittivity, $\chi^{(1)}$, and $\chi^{(2)}$ and $\chi^{(3)}$ are the first, second and third-order nonlinear susceptibilities. OPAs are optical amplifiers based on the $\chi^{(2)}$ nonlinearity of a crystal,[6–8] in a process, called parametric,[6,7] where there is no net transfer of energy and momentum between E and the crystal.[6,7] This can be visualized by considering energy transfer from a pump pulse of frequency ω_p to two pulses of lower frequencies ω_s and ω_i, called signal and idler,[6,7] with the requirement $\omega_p = \omega_s + \omega_i$.[6,7] Under this condition, OPAs can transfer energy form a narrow, fixed $\Delta\lambda$, pump pulse, to a broad, variable $\Delta\lambda$, signal pulse, e.g., from ~600 to over 3500 nm, with pulses shorter than 3-cycles,[2,9] their duration being ultimately limited by uncompensated dispersive and nonlinear effects.[2,9] However, both Ti:Sapphire oscillators and OPAs optimized to produce few-cycle pulses are complex and expensive setups, relying on bulk optics.[2,9] This has driven a research effort to find novel approaches, not only capable of producing short pulses, but also cost-effective, simple, broadband, and inexpensive, which would make few-cycle pulses more accessible.

Compared to their solid-state counterparts, fiber lasers are attractive platforms for short pulse generation due to their simple and compact designs,[10] efficient heat dissipation,[11] and alignment-free operation.[1,2,11] These characteristics, combined with advances in glass technology[12,13] and nonlinear optics,[14] has resulted in systems working from the visible to the mid-infrared (MIR).[12] In fiber oscillators, ultrashort pulses can be obtained by passive mode-locking.[10] This typically requires the aid of a non-linear component, called saturable absorber (SA).[1,3,10] Graphene[15,16] and carbon nanotubes (CNTs)[15,17,18] have emerged as promising SAs for ultrafast lasers.[16,17,19–25] In CNTs, broadband operation is achieved by using a distribution of tube diameters,[17,20] while this is an intrinsic property of graphene.[26] This, along with the ultrafast recovery time,[27] low saturation fluence,[16,28] and ease of fabrication[29] and integration,[30] makes graphene an excellent broadband SA.[26] Consequently, mode-locked lasers using graphene SAs (GSAs) have been demonstrated from ~800 nm[31] to ~970 nm,[32] ~1 μm,[33] ~1.5 μm,[26] ~2μm,[34] and ~2.5μm.[35] Therefore, experimental setups that combine the unique optical properties and simple fabrication of graphene, with fiber lasers, are attractive prospects for few-cycle pulse generation.

For fiber lasers, a typical approach for ultrashort pulse generation is soliton mode-locking.[1,2] In this regime, the fiber dispersive and non-linear effects can cancel each other,[1,2] allowing a stable pulse envelope to propagate.[1,2] During propagation, the soliton periodically encounters perturbations occurring in the fiber laser of cavity length (L_c).[36]

a)Electronic mail: dp387@cam.ac.uk

 © 2015 AIP Publishing LLC

This article is copyrighted as indicated in the article. Reuse of AIP content is subject to the terms at: http://scitation.aip.org/termsconditions. Downloaded to IP: 129.169.173.200 On: Mon, 29 Jun 2015 16:19:24

The shortest solitons stably supported by the cavity have typically $Z_0 < \frac{L_c}{2}$, where $Z_0 \simeq \frac{\Delta\tau^2}{2\beta^{(2)}}$ is the soliton period with $\beta^{(2)}$ the second-order dispersion.[37] For pulses with $\Delta\tau < 100$ fs, one needs $L_c < \frac{\Delta\tau^2}{\beta^{(2)}} \simeq 40$ cm for fiber lasers operating at 1.5 μm, where $\beta^{(2)} \simeq -25\,\mathrm{ps}^2/\mathrm{km}$. For such short L_c, it becomes challenging to compensate dispersive effects in all-fiber formats,[36] e.g., to achieve ~10-cycle pulses, i.e. ~30 fs at 1 μm,[38–40] the shortest reported to date,[39,40] bulk optics are typically employed[38–40] in order to compensate for dispersive effects, eliminating the advantage of alignment-free operation. A strategy to overcome these limitations in all-fiber laser formats is to use a dispersion-managed cavity design,[37,41] where alternating segments of positive (or normal) and negative (or anomalous) dispersion fibers lead to periodic broadening and compression of the intracavity pulses.[37,41] Compared to soliton mode-locking, the average $\Delta\tau$ can increase by an order of magnitude or more, which significantly reduces the intracavity peak power (P_{peak}), thus being less susceptible to nonlinear optical effects.[37,41] However, in all-fiber oscillators, it is difficult to achieve the minimum $\Delta\tau$, as set by T_0. Dispersive effects increase with $\Delta\lambda$, and it is necessary to provide compensation for orders higher than $\beta^{(2)}$, e.g., third-order dispersion $\beta^{(3)}$ or even higher.[36] In addition, the limited operating $\Delta\lambda$ of gain fibers, typically ~50 nm,[12] can further limit the minimum achievable $\Delta\tau$.

A different route for few-cycle pulse generation is to externally compress the pulse.[2,36] In this approach, the pulse is first passed through a non-linear medium, such as a length of single mode fiber (SMF),[36] where it experiences self-induced phase modulation (SPM) (non-linear phase delay),[2,36] caused by its own intensity $I(t)$, via the Kerr effect,[36] i.e., $I(t)$-dependent change in the refractive index $\Delta n = n_2 I(t)$, where n_2 is the medium nonlinear index coefficient.[36] After a propagation length L, the pulse accumulates a time dependent phase-shift $\Delta\phi(t) = \frac{2\pi\nu_0 n_2 I(t) L}{c}$,[36] resulting in the generation of new frequency components $\Delta\nu(t) = \frac{1}{2\pi}\frac{d\Delta\phi(t)}{dt}$,[2,36] distributed temporally across the pulse, i.e., the pulse becomes chirped. In order to achieve shorter $\Delta\tau$, as supported by the now broadened $\Delta\nu$, the chirped pulse is then passed through a dispersive delay line,[36] which re-phases the new frequency components, $\Delta\nu(t)$, generated by the SPM.[2,36] Ideally, the dispersive delay line would introduce the inverse of the chirp added by SPM, resulting in the compression of the pulse to its minimum duration. Typically, the dispersive delay line, formed by a component with negative dispersion, compensates for the linear chirp, around the central part of the pulse, where most energy is concentrated.[2,36] When compared to other techniques, such as OPAs, external pulse compression offers a more flexible design,[2] with the possibility of taking advantage of the ultra-broadband spectrum, which can be generated by SPM processes[2,36] in all-fiber formats.[36] Using this approach, various fiber based laser configurations have been investigated for few-cycle pulse generation. E.g., Ref. 42 demonstrated ~20 fs pulses using a commercial passively mode-locked laser in conjunction with a similariton amplifier,[42] while Ref. 43 achieved ~7.8 fs, using an erbium-doped fiber laser (EDFA) oscillator and amplifier in conjunction with a highly nonlinear fiber to achieve an ultrabroadband spectrum, followed by compression.[43] Pulses approaching the single-cycle regime have been demonstrated by combining two separate ultrabroadband spectra, by dividing the output from a single EDFA oscillator,[44] to produce a single spectrum spanning 900–2100 nm with ~4.3 fs pulses.[44] Although these results are close to single-cycle,[44] their practical application is hindered by the setup complexity, such as the use of bulk optics.[43,44] Thus, of particular interest are novel setups, still capable of few-cycle pulse generation, but with simpler, more accessible designs, and ampler operation wavelength, while maintaining the all-fiber format.

Here, we achieve ~29 fs pulses, corresponding to less than 6-cycles at 1550 nm, using a graphene mode-locked fiber oscillator in conjunction with an external compressor based on an EDFA and a length of SMF. The EDF length within the amplifier acts as the gain and non-linear medium, used to simultaneously amplify and spectrally broaden the pulse, while the SMF, placed at the output of the EDFA, acts as the dispersive delay line. Our design uses only standard telecommunication equipment and an intrinsic broadband GSA, attractive when low cost, ease of fabrication, and operational stability are required. In addition, this enables a compact and portable format.

We use a graphene polyvinyl alcohol (PVA) composite as our GSA, fabricated via solution processing. Graphene flakes are exfoliated from bulk graphite by mild ultrasonication with sodium deoxycholate (SDC) surfactant.[16,30] A dispersion enriched with single layer (SLG) and few layer graphene is then mixed with an aqueous solution of PVA. After water evaporation, a ~50 μm thick graphene-PVA composite is obtained.[16] The optical absorption measurements of the graphene-PVA composite are presented in Fig. 1(a). We estimate the number of graphene layers (N) in the composite from the absorption measurements by using the transfer matrix formalism,[45] assuming that SLG absorbs 2.3%.[46] We calculate, as a function of N, the absorption of a graphene-PVA composite with overall thickness corresponding to the experimental one, and with graphene layers randomly distributed within the matrix. The graphene refractive

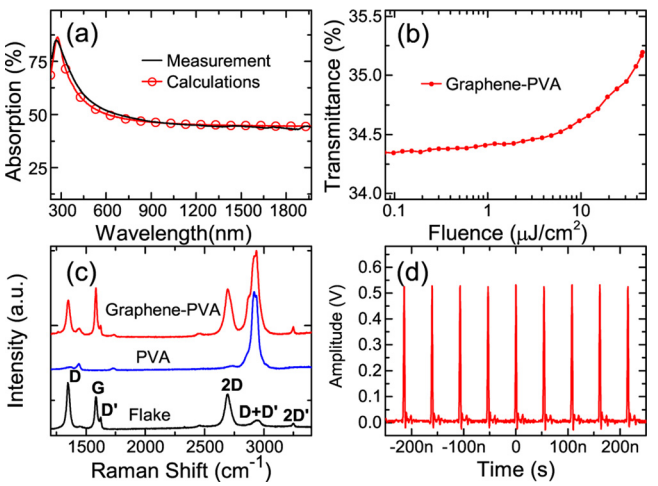

FIG. 1. (a) Calculated and measured absorption of graphene-PVA composite. (b) Nonlinear transmittance of graphene-PVA composite. (c) 514.5 nm Raman spectra of a graphene flake, PVA reference, and graphene-PVA composite. (d) Oscilloscope trace.

This article is copyrighted as indicated in the article. Reuse of AIP content is subject to the terms at: http://scitation.aip.org/termsconditions. Downloaded to IP: 129.169.173.200 On: Mon, 29 Jun 2015 16:19:24

index is taken from ellipsometric measurements,[47] while the PVA refractive index is adjusted to reproduce the experimental reflectivity measured on the pure polymer film: ~1.44.[48] In order to avoid coherent multiple reflections due to a specific arrangement of the graphene layers in the composite, we perform a statistical sampling by repeating the calculations for ~2000 random graphene distributions within the film. By comparing our calculations with the experimental absorption, Fig. 1(a), we estimate that a 43% overall absorption translates to N ~30–35. The nonlinear optical transmittance is measured with an optical parametric oscillator (Coherent, Chameleon) delivering ~200 fs pulses with 4 MHz repetition rate at $\lambda_0 = 1550$ nm. The optical transmittance is determined by monitoring the input and output power on the GSA and presented in Fig. 1(b). The transmittance increases from ~34.3% to ~35.3%, a change of ~1%, typical of GSAs.[16,28] Fig. 1(c) plots the Raman spectra of a graphene flake deposited on Si/SiO_2, the PVA reference, and the graphene-PVA composite. Besides the G and 2D peaks, the Raman spectrum of the flake has significant D and D′ intensities.[49,50] We assign the D and D′ peaks to the edges of the submicrometer flakes,[51] rather than a large amount of disorder within the flakes.[52] This is further supported by analyzing the G peak dispersion, Disp(G). In disordered carbons, Pos(G) increases with decreasing excitation wavelength, from infrared to ultraviolet.[50] Thus, Disp(G) increases with disorder.[50,53] FWHM(G) always increases with disorder.[54] Hence, combining the intensity ratio of the D and G peaks, I(D)/I(G), with FWHM(G) and Disp(G) allows us to discriminate between edges, and disorder in the bulk of the samples. In the latter case, a higher I(D)/I(G) would correspond to higher FWHM(G) and Disp(G). By analyzing 30 flakes, we find that Disp(G), I(D)/I(G), and FWHM(G) are not correlated, indicating that the D peak is mostly due to edges. Also, Disp(G) is nearly zero for all samples (compared to $\geq 0.1\,cm^{-1}/nm$ expected for disordered carbons[53]). Although 2D is broader than in pristine graphene, it is still a single Lorentzian. This implies that, even if the flakes are multilayers, they are electronically decoupled and, to a first approximation, behave as a collection of single layers.[55] The spectrum of the composite (Fig. 1(c)) can be seen as a superposition of those of a flake and of PVA. Thus, PVA does not affect the structure of the embedded flakes.

For our seed oscillator, we design a dispersion-managed soliton setup,[28] able to generate shorter $\Delta\tau$, with broader $\Delta\lambda$ than soliton lasers,[41] schematically presented in Fig. 2(a). The total cavity length is $L_c \sim 11$ m. We use a $L_1 \sim 3.7$ m EDF, with $\beta_1^{(2)} \sim 23\,ps^2/km$ as gain medium. The EDF is pumped by a 980 nm continuous wave (CW) laser diode (LD) through a fused wavelength division multiplexer (WDM). The rest of the cavity is formed from two lengths of standard SMF: $L_2 \sim 6.9$ m of SMF-28 with $\beta_2^{(2)} \sim -22\,ps^2/km$ and $L_3 \sim 40$ cm of Flexcore-1060 with $\beta_3^{(2)} \sim -7\,ps^2/km$. This gives a net intracavity second-order dispersion $L_1\beta_1^{(2)} + L_2\beta_2^{(2)} + L_3\beta_3^{(2)} \sim -0.07\,ps^2$, typical of dispersion-managed soliton lasers.[19,28] The output of the cavity is the 30% port of a 70/30 coupler. The lasing threshold is ~12 mW. The GSA is then sandwiched between two fiber connectors[28] and placed after the coupler. Passive, fundamental mode-locking is achieved with the aid of the GSA with an output power $P_{out} = 0.68$ mW, corresponding to ~20 mW pump power. The oscilloscope trace corresponding to a repetition rate of $f_1 = 18.67$ MHz, is presented in Fig. 1(d), showcasing the single pulse operation. The seed pulse optical spectrum is shown in Fig. 3(a), with a spectral width $\Delta\lambda_s = 10.4$ nm. The corresponding intensity autocorrelation

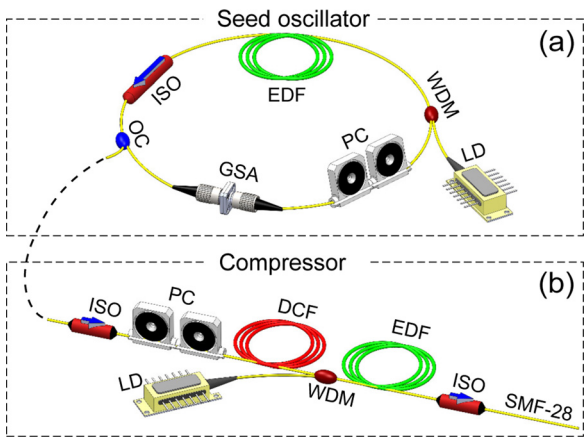

FIG. 2. Laser schematic. The seed oscillator (a) is mode-locked using a GSA to produce 263 fs seed pulses. These are fed through the compressor (b), reducing their duration down to 29 fs. LD: Laser diode; WDM: Wavelength division multiplexer; EDF: Erbium doped fiber; ISO: Isolator; OC: Optical coupler; PC: Polarization controller; DCF: Dispersion compensating fiber; and SMF: Single mode fiber.

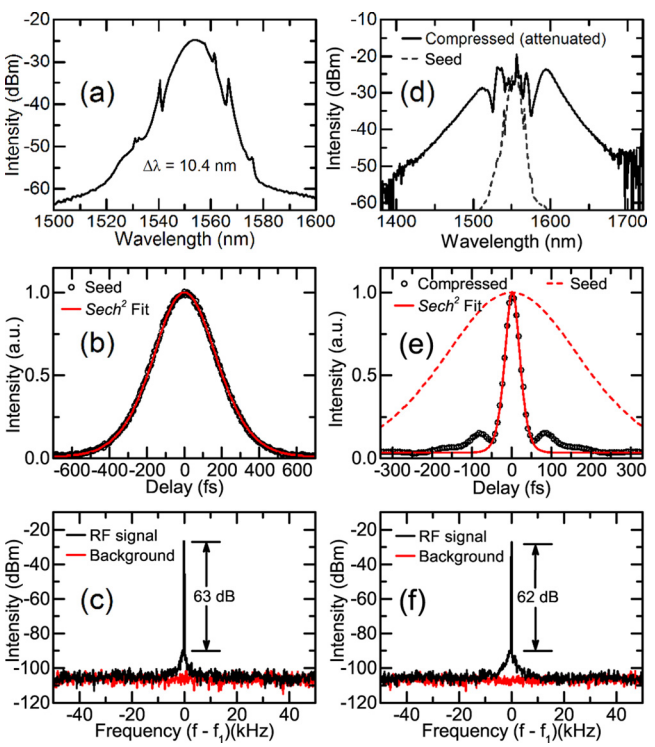

FIG. 3. Pulse characterisation before (left) and after (right) compression. (a) Optical spectra, with $\Delta\lambda_s = 10.4$ nm. (b) Intensity autocorrelation trace fitted with a $sech^2$ profile, giving $\Delta\tau_s = 263$ fs after deconvolution. (c) RF spectrum showing the first harmonic, measured around $f_1 = 18.67$ MHz with a 100 kHz span and 30 Hz resolution. (d) Optical spectra. (e) Intensity autocorrelation trace, fitted with a $sech^2$ profile. Both seed and compressed traces are normalized to 1. (f) RF spectrum, after attenuation to ~1.5 mW to avoid damage to the photodetector, showing the first harmonic at 18.67 MHz, with a 100 kHz span and 30 Hz resolution.

This article is copyrighted as indicated in the article. Reuse of AIP content is subject to the terms at: http://scitation.aip.org/termsconditions. Downloaded to IP: 129.169.173.200 On: Mon, 29 Jun 2015 16:19:24

trace is shown in Fig. 3(b), with duration $\Delta\tau_s = 263$ fs, as determined by fitting a $sech^2$ profile to the pulse, as expected for soliton-like mode-locking.[36] This gives a time bandwidth product (TBP) $\Delta\nu_s\Delta\tau_s = 0.34$, close to the expected transform-limit 0.315, where $\Delta\nu_s$ is the oscillator frequency bandwidth.[56] Our oscillator is comparable to current state-of-art graphene[28,57,58] and CNT[19,57,59] based fiber oscillators.

The design of the compressor is based on an EDFA, as shown in Fig. 2(b). To protect against back reflections,[60] two isolators are placed at both the input and output, consisting of ~40 and ~50 cm of SMF-28. To reduce P_{peak} and avoid temporal pulse-shape distortions[1] or damage to the compressor components,[1] we stretch the pulse using ~3.6 m of dispersion compensating fiber (DCF) with $\beta^{(2)} \sim 60\,ps^2/km$, after the input isolator. After the DCF, a WDM consisting of ~220 cm Flexcore-1060 is used to forward pump ~3 m of EDF with $\beta^{(2)} \sim 17\,ps^2/km$, employed as the gain medium. A length of SMF-28, placed after the EDF, forms the dispersive delay line, for which an optimized length ~125 cm (including the ~50 cm output isolator) is used, as determined by monitoring the autocorrelation trace at the compressor output until a minimum in the pulse duration is achieved. A polarization controller (PC) is utilized to match the polarization state of the incident seed pulses (compression optimization).

The EDFA within the compressor is operated with a pump power $P_{pump} \sim 350$ mW. Fig. 3(d) plots the optical spectrum recorded at the output of the compressor, with spectral width $\Delta\lambda_c$. $\Delta\lambda_c > 100$ nm indicates that spectral broadening has occurred. The corresponding intensity autocorrelation trace is shown in Fig. 3(e), with a $sech^2$ profile with duration $\Delta\tau_c \sim 29$ fs, i.e., ~6 optical cycles. This gives a compression factor $\frac{\Delta\tau_s}{\Delta\tau_c} = 9$. The radio frequency (RF) spectrum of the pulse train, measured with a photodetector connected to a RF spectrum analyzer, is reported in Figs. 3(c) and 3(f), before and after compression, respectively. Relative to the seed pulses, the compressed pulses have no degradation in signal-to-noise ratio (SNR), indicating that pulse stability is maintained during compression.[61] After compression, $P_{out} = 52$ mW corresponding to a pulse energy $E_{pulse} = 2.8$ nJ. An increased pedestal is observed at the base of the pulse, which can be attributed to uncompressed non-linear chirp added to the pulse through SPM.[36] Compensation of higher order chirp terms would enable further reduction in pulse duration,[2,36] as well as minimization of the pedestal structure at the base of the pulse.[36] This can be achieved through control of the higher order dispersion terms within the dispersive delay line, e.g., to control $\beta^{(3)}$,[36] prism pairs or chirped mirrors,[2] or lengths of photonic crystal fibers (PCFs),[13] could be used. The amount of spectral broadening achievable with our setup, therefore the minimum supported pulse duration, is further limited by the maximum P_{pump} of the laser diode used to pump the EDFA. Use of a higher power diode, or a double pumped configuration, should enable the generation of higher bandwidth pulses, as well as enabling increased output power. Finally, wavelength-engineered dispersion management, e.g., using PCFs,[13] coupled with the broadband nature of graphene,[26] could, in principle, extend our approach to enable short pulses at other wavelengths.

Compared to Ti:Sapphire and OPA designs, we use all-fiber components, that are simple to assemble and need no critical alignment. A CNT-based fiber setup capable of ~14 fs pulses at 1550 nm was reported in Ref. 62. Despite the shorter pulses, Ref. 62 used bulk optics (a prism pair),[62] unlike the alignment-free all-fiber format of our laser. Also, a CNT-based SA limits the operation wavelength, compared to our GSA, that can operate at any wavelength.

In conclusion, we reported a graphene-mode locked laser generating 29 fs pulses with an average output power ~52 mW and pulse energy 2.8 nJ, making it attractive for applications such as optical frequency comb generation and high resolution spectroscopy.

We acknowledge funding from EU Graphene Flagship (No. 604391), ERC Grant Hetero2D, EPSRC Grant Nos. EP/K01711X/1, EP/K017144/1, EP/M507799/1, and EP/L016087/1, a Royal Society Wolfson Research Merit Award, and Emmanuel College, Cambridge.

[1]M. E. Fermann, A. Galvanauskas, and G. Sucha, *Ultrafast Lasers: Technology and Applications* (CRC Press, 2003).
[2]F. X. Kärtner, *Few-Cycle Laser Pulse Generation and Its Applications* (Springer, 2004).
[3]U. Keller, Nature **424**, 831 (2003).
[4]R. Ell, U. Morgner, F. X. Kartner, J. G. Fujimoto, E. P. Ippen, V. Scheuer, G. Angelow, T. Tschudi, M. J. Lederer, A. Boiko, and B. Luther-Davies, Opt. Lett. **26**, 373 (2001).
[5]See http://www.coherent.com/download/6416/Chameleon-Ultra-Family-Data-Sheet.pdf for a commercially available tunable Ti:Sapphire ultrafast oscillator.
[6]R. W. Boyd, *Nonlinear Optics*, 3rd ed. (Academic Press, 2008).
[7]R. L. Sutherland, D. G. McLean, and S. Kirkpatrick, *Handbook of Nonlinear Optics* (Marcel Dekker, New York, 2003).
[8]G. Cerullo and S. De Silvestri, Rev. Sci. Instrum. **74**, 1 (2003).
[9]D. Brida, C. Manzoni, G. Cirmi, M. Marangoni, S. Bonora, P. Villoresi, S. D. Silvestri, and G. Cerullo, J. Opt. **12**, 013001 (2010).
[10]M. E. Fermann and I. Hartl, Nat. Photonics **7**, 868 (2013).
[11]F. Dausinger, F. Lichtner, and H. Lubatschowski, *Femtosecond Technology for Technical and Medical Applications* (Springer, Berlin, 2004).
[12]M. J. F. Digonnet, *Rare Earth Doped Fiber Lasers and Amplifiers* (Marcel Dekker, NY, USA, 1993).
[13]P. Russell, Science **299**, 358 (2003).
[14]J. M. Dudley and J. R. Taylor, Nat. Photonics **3**, 85 (2009).
[15]T. Hasan, Z. Sun, F. Wang, F. Bonaccorso, P. H. Tan, A. G. Rozhin, and A. C. Ferrari, Adv. Mater. **21**, 3874 (2009).
[16]Z. Sun, T. Hasan, F. Torrisi, D. Popa, G. Privitera, F. Wang, F. Bonaccorso, D. M. Basko, and A. C. Ferrari, ACS Nano **4**, 803 (2010).
[17]F. Wang, A. G. Rozhin, V. Scardaci, Z. Sun, F. Hennrich, I. H. White, W. I. Milne, and A. C. Ferrari, Nat. Nanotechnol. **3**, 738 (2008).
[18]V. Scardaci, Z. P. Sun, F. Wang, A. G. Rozhin, T. Hasan, F. Hennrich, I. H. White, W. I. Milne, and A. C. Ferrari, Adv. Mater. **20**, 4040 (2008).
[19]D. Popa, Z. Sun, T. Hasan, W. Cho, F. Wang, F. Torrisi, and A. Ferrari, Appl. Phys. Lett. **101**, 153107 (2012).
[20]R. Going, D. Popa, F. Torrisi, Z. Sun, T. Hasan, F. Wang, and A. C. Ferrari, Physica E **44**, 1078 (2012).
[21]C. E. S. Castellani, E. J. R. Kelleher, D. Popa, T. Hasan, Z. Sun, A. C. Ferrari, S. V. Popov, and J. R. Taylor, Laser Phys. Lett. **10**, 015101 (2013).
[22]M. Zhang, E. J. R. Kelleher, T. H. Runcorn, V. M. Mashinsky, O. I. Medvedkov, E. M. Dianov, D. Popa, S. Milana, T. Hasan, Z. Sun *et al.* Opt. Express **21**, 23261 (2013).
[23]R. I. Woodward, E. J. R. Kelleher, D. Popa, T. Hasan, F. Bonaccorso, A. C. Ferrari, S. V. Popov, and J. R. Taylor, IEEE Photonics Technol. Lett. **26**, 1672 (2014).
[24]D. Popa, Z. Sun, T. Hasan, F. Torrisi, F. Wang, and A. C. Ferrari, Appl. Phys. Lett. **98**, 073106 (2011).
[25]Z. Sun, D. Popa, T. Hasan, F. Torrisi, F. Wang, E. J. R. Kelleher, J. C. Travers, V. Nicolosi, and A. C. Ferrari, Nano Res. **3**, 653 (2010).

This article is copyrighted as indicated in the article. Reuse of AIP content is subject to the terms at: http://scitation.aip.org/termsconditions. Downloaded to IP: 129.169.173.200 On: Mon, 29 Jun 2015 16:19:24

[26]F. Bonaccorso, Z. Sun, T. Hasan, and A. C. Ferrari, Nat. Photonics **4**, 611 (2010).
[27]D. Brida, A. Tomadin, C. Manzoni, Y. J. Kim, A. Lombardo, S. Milana, R. R. Nair, K. S. Novoselov, A. C. Ferrari, G. Cerullo, and M. Polini, Nat. Commun. **4**, 1987 (2013).
[28]D. Popa, Z. Sun, F. Torrisi, T. Hasan, F. Wang, and A. C. Ferrari, Appl. Phys. Lett. **97**, 203106 (2010).
[29]A. C. Ferrari, F. Bonaccorso, V. Falko, K. S. Novoselov, S. Roche, P. Boggild, S. Borini, F. Koppens, V. Palermo, N. Pugno *et al.*, Nanoscale **7**, 4598 (2015).
[30]F. Bonaccorso, A. Lombardo, T. Hasan, Z. P. Sun, L. Colombo, and A. C. Ferrari, Mater. Today **15**, 564 (2012).
[31]I. H. Baek, H. W. Lee, S. Bae, B. H. Hong, Y. H. Ahn, D.-I. Yeom, and F. Rotermund, Appl. Phys. Express **5**, 032701 (2012).
[32]C. A. Zaugg, Z. Sun, V. J. Wittwer, D. Popa, S. Milana, T. S. Kulmala, R. S. Sundaram, M. Mangold, O. D. Sieber, M. Golling, Y. Lee, J. H. Ahn, A. C. Ferrari, and U. Keller, Opt. Express **21**, 31548 (2013).
[33]R. Mary, S. J. Beecher, G. Brown, F. Torrisi, S. Milana, D. Popa, T. Hasan, Z. Sun, E. Lidorikis, S. Ohara, A. C. Ferrari, and A. K. Kar, Opt. Express **21**, 7943 (2013).
[34]M. Zhang, E. J. R. Kelleher, F. Torrisi, Z. Sun, T. Hasan, D. Popa, F. Wang, A. C. Ferrari, S. V. Popov, and J. R. Taylor, Opt. Express **20**, 25077 (2012).
[35]M. N. Cizmeciyan, J. W. Kim, S. Bae, B. H. Hong, F. Rotermund, and A. Sennaroglu, Opt. Lett. **38**, 341 (2013).
[36]G. P. Agrawal, *Applications of Nonlinear Fiber Optics* (Academic Press, London, 2001).
[37]K. Tamura, E. P. Ippen, H. A. Haus, and L. E. Nelson, Opt. Lett. **18**, 1080 (1993).
[38]J. R. Buckley, S. W. Clark, and F. W. Wise, Opt. Lett. **31**, 1340 (2006).
[39]X. Zhou, D. Yoshitomi, Y. Kobayashi, and K. Torizuka, Opt. Express **16**, 7055 (2008).
[40]D. Ma, Y. Cai, C. Zhou, W. Zong, L. Chen, and Z. Zhang, Opt. Lett. **35**, 2858 (2010).
[41]L. E. Nelson, D. J. Jones, K. Tamura, H. A. Haus, and E. P. Ippen, Appl. Phys. B **65**, 277 (1997).
[42]B. Kibler, C. Billet, P. A. Lacourt, R. Ferriere, and J. M. Dudley, IEEE Photonics Technol. Lett. **18**, 1831 (2006).
[43]A. Sell, G. Krauss, R. Scheu, R. Huber, and A. Leitenstorfer, Opt. Express **17**, 1070 (2009).
[44]G. Krauss, S. Lohss, T. Hanke, A. Sell, S. Eggert, R. Huber, and A. Leitenstorfer, Nat. Photonics **4**, 33 (2010).
[45]M. Born and E. Wolf, *Principles of Optics: Electromagnetic Theory of Propagation, Interference and Diffraction of Light* (Cambridge University Press, Cambridge, 1999).
[46]R. R. Nair, P. Blake, A. N. Grigorenko, K. S. Novoselov, T. J. Booth, T. Stauber, N. M. R. Peres, and A. K. Geim, Science **320**, 1308 (2008).
[47]V. G. Kravets, A. N. Grigorenko, R. R. Nair, P. Blake, S. Anissimova, K. S. Novoselov, and A. K. Geim, Phys. Rev. B **81**, 155413 (2010).
[48]N. P. Cheremisinoff, *Handbook of Engineering Polymeric Materials* (Marcel Dekker, New York, 1997).
[49]A. C. Ferrari, J. C. Meyer, V. Scardaci, C. Casiraghi, M. Lazzeri, F. Mauri, S. Piscanec, D. Jiang, K. S. Novoselov, S. Roth, and A. K. Geim, Phys. Rev. Lett. **97**, 187401 (2006).
[50]A. C. Ferrari and J. Robertson, Phys. Rev. B **61**, 14095 (2000).
[51]F. Torrisi, T. Hasan, W. Wu, Z. Sun, A. Lombardo, T. S. Kulmala, G.-W. Hsieh, S. Jung, F. Bonaccorso, P. J. Paul, D. Chu, and A. C. Ferrari, ACS Nano **6**, 2992 (2012).
[52]C. Casiraghi, A. Hartschuh, H. Qian, S. Piscanec, C. Georgi, A. Fasoli, K. S. Novoselov, D. M. Basko, and A. C. Ferrari, Nano Lett. **9**, 1433 (2009).
[53]A. C. Ferrari and J. Robertson, Phys. Rev. B **64**, 075414 (2001).
[54]L. G. Cancado, A. Jorio, E. H. M. Ferreira, F. Stavale, C. A. Achete, R. Capaz, M. Moutinho, A. Lombardo, T. S. Kulmala, and A. C. Ferrari, Nano Lett. **11**, 3190 (2011).
[55]S. Latil, V. Meunier, and L. Henrard, Phys. Rev. B **76**, 201402 (2007).
[56]U. Keller, *Progress in Optics* (Elsevier, 2004), Vol. 46, p. 1.
[57]A. Martinez and Z. Sun, Nat. Photonics **7**, 842 (2013).
[58]H. Zhang, D. Tang, R. J. Knize, L. Zhao, Q. Bao, and K. P. Loh, Appl. Phys. Lett. **96**, 111112 (2010).
[59]T. Hasan, Z. Sun, P. Tan, D. Popa, E. Flahaut, E. J. R. Kelleher, F. Bonaccorso, F. Wang, Z. Jiang, F. Torrisi, G. Privitera, V. Nicolosi, and A. C. Ferrari, ACS Nano **8**, 4836 (2014).
[60]M. Becker, A. Olsson, and J. Simpson, *Erbium-Doped Fiber Amplifiers: Fundamentals and Technology* (Academic Press, 1999).
[61]D. V. D. Linde, Appl. Phys. B: Lasers Opt. **39**, 201 (1986).
[62]K. Kieu, R. J. Jones, and N. Peyghambarian, IEEE Photonics Technol. Lett. **22**, 1521 (2010).

This article is copyrighted as indicated in the article. Reuse of AIP content is subject to the terms at: http://scitation.aip.org/termsconditions. Downloaded to IP: 129.169.173.200 On: Mon, 29 Jun 2015 16:19:24